Environmental Health Perspectives
Vol. 9, pp. 63–80, 1974

Electron Microscopical Investigation of Asbestos Fibers

by Arthur M. Langer,* Anne D. Mackler,* and Fred D. Pooley †

Examination of asbestos fibers by electron microscopical techniques enables the observer to distinguish among the fiber types by morphological and structural characteristics.

Chrysotile asbestos fibers are composed of bundles of fibrils. Fibers are often curvilinear with splayed ends. Individual fibrils consist of a central capillary defined by an electron dense crystalline wall. With increasing time of electron bombardment, the capillary wall decreases in thickness, deforms, and is encapsulated in an electron translucent material. The change in electron opacity is considered to be a product of structural disruption brought about by dehydroxylation due to electron radiation. A well recognized sequential deformation pattern may be used for identification purposes.

Amphibole fibers tend to be straight, splintery, and electron-opaque, although curved fibers are occasionally observed. Diffraction contrast figures are visible as dark bands moving parallel and at right angles to the fiber axis. Crocidolite forms the shortest and thinnest fibers, followed in size by amosite and anthophyllite. Size distribution characteristics of the amphibole fiber types are different.

The selected area electron diffraction pattern for chrysotile is unique. Reflections range in forms from streaked to arcuate. Reflection intensity and shape are related to the degree of openness of the fiber bundle and the extent of physical degradation of the fiber. The amphibole asbestos fibers possess diffraction patterns having similar characteristics prohibiting individual identification. Microchemical analysis is required for identification in such cases.

A discussion of the industrial hygiene threshold limit values for ampliphibole asbestos fibers is presented. The discussion is based on their differing size distribution characteristics.

Introduction

The biological effects of asbestos in the workplace have been defined *(1)*. In occupational settings, where indirect fiber exposure is common, as in shipyards, an ever-increasing body of evidence indicates that hazards exist, albeit to a lesser degree than in direct occupational contact *(2)*. The most intriguing, if not the most important, asbestos problem deals with the families of asbestos workmen, populations living around the epicenters of asbestos mining, milling, and manufacturing operations, and the use of asbestos products by the general population. Scientific inquiry is now focusing on how far into the general population the disease hazard is manifest *(3)*. This latter question may be answered, in part, with proper epidemiological study. However, in such circumstances, the definition of fiber exposure is crucial.

The monitoring of working environments presents few problems in terms of defining the nature of the fiber used. That is, the working environment provides sufficient material for analysis and latitude in the selection of analytical technique. Fiber characterization is readily achieved *(4)*. In those areas removed from defined fiber exposure, the problem connected with dust characterization may be enor-

*Environmental Sciences Laboratory, The Mount Sinai School of Medicine of the City University of New York, New York, 10029.

†Department of Mineral Exploitation, University College of South Wales and Monmouthshire, Cardiff, Wales.

mous. Removed from the occupational setting, sublight microscopic fibers, often few in number, predominate. In these instances identification of single fibers may be required. It is the purpose of this paper to describe briefly some of the characteristics of sublight microscopic asbestos fibers which may be used for identification and characterization of small numbers of or even single asbestos fibers.

Asbestos Minerals

The asbestos minerals are naturally occurring hydrated silicates which form fibers on comminution. Their commercial properties are many and have been described in detail *(5)*. Asbestos fibers belong to two mineral groups both of which possess molecular configurations and structures predetermining the development of fiber morphology. Chrysotile, the serpentine rolled sheet silicate, forms cylindrical fibrils because of the structural mismatch between the component brucite and silica sheets *(6)*.

The asbestos types amosite, anthophyllite, crocidolite, and tremolite belong to the amphibole mineral class in which cations link $Si_8O_{22}(OH)_2$ groups to form an infinite chain which constitutes the fiber axis. The chemistry and structure of these mineral forms has been described elsewhere *(7)*.

As a point of caution, mineral names themselves are misleading. Any one mineral species may vary in both chemical and physical properties. Therefore, the asbestos names cited in the literature may represent a wide range of materials *(8)*. This paper will describe the morphology and selected area electron diffraction characteristics of selected asbestos fibers.

Experimental

Materials

The UICC standard reference asbestos minerals were used to provide specimens of anthophyllite, amosite, and crocidolite *(9)*. Tremolite was obtained from the vermiculite pit mining operation at Libby, Montana (sample provided by W. Bank, U.S. Bureau of Mines, Denver, Colo.). Chrysotile samples from the Jeffrey mine, Asbestos, Quebec, were obtained and used as the principal representative of this fiber type (sample provided by S. Speil, Johns-Manville Corp., Denver Research Center, Denver, Colo.).

Preparation

The different amphibole asbestos minerals (0.1 mg) were placed in glass tubes and immersed in distilled water (5.0 ml). This material was manually agitated for 30 sec. The suspensions were further dispersed with ultrasonic activity for 60 sec (Sonifier Cell Disrupter, Heat Systems-Ultrasonics Inc. Model W185D).

A 1 μl aliquot, withdrawn from the bottom of each suspension was pipetted onto carbon-coated Formvar grids and allowed to evaporate to dryness. The grids were carbon-coated again to form a sandwich around the particles. Chrysotile asbestos was prepared from an open, triple air-jet milled sample in a similar manner. The samples were examined by transmission electron microscopy with accelerating voltage set at 120 kV and 100 kV. Two instruments were used: Hitachi HU 11E-125; and a JEOL JEM 120U. Scan magnification varied from 1500× to 40,000× in each case. At least 50 areas on several grids were inspected to assure homogeneity of sample preparation. Representative areas of each preparation were photographed.

Results and Discussion

Morphology of Amphibole Asbestos Fibers

Examination of amphibole asbestos fibers demonstrates one morphological characteristic that is common to all at low magnification. Individual fibers tend to form straight, electron-dense to opaque fibers. At magnifications less than 3000×, the population of each fiber type displays remarkably different fiber lengths and widths (Fig. 1). In addition to straight fibers, curved fibers are occasionally observed (Fig. 2). Crocidolite appears to form curved fibers more often than the other amphibole asbestos types. In all cases, the thinnest fibers predominate in the curved population. Amphibole fibers tend to form morphologically straight edges parallel to the fiber axis but irregular edges are observed as well (Fig. 3). These irregularities may be related to both cleavage and fracture. Ends of

FIGURE 1. Transmission electron micrographs of representative fields of *(A)* crocidolite; *(B)* amosite; *(C)* anthophyllite. Fibers tend toward straight splinters and electron opacity. General impression: crocidolite forms smallest particles, amosite larger particles, anthophyllite the largest particles. Anthophyllite sample is contaminated with talc plates. Bar marks in *(A)* and *(B)* equal 0.5 μm. Magnification in *B* and *C* is the same.

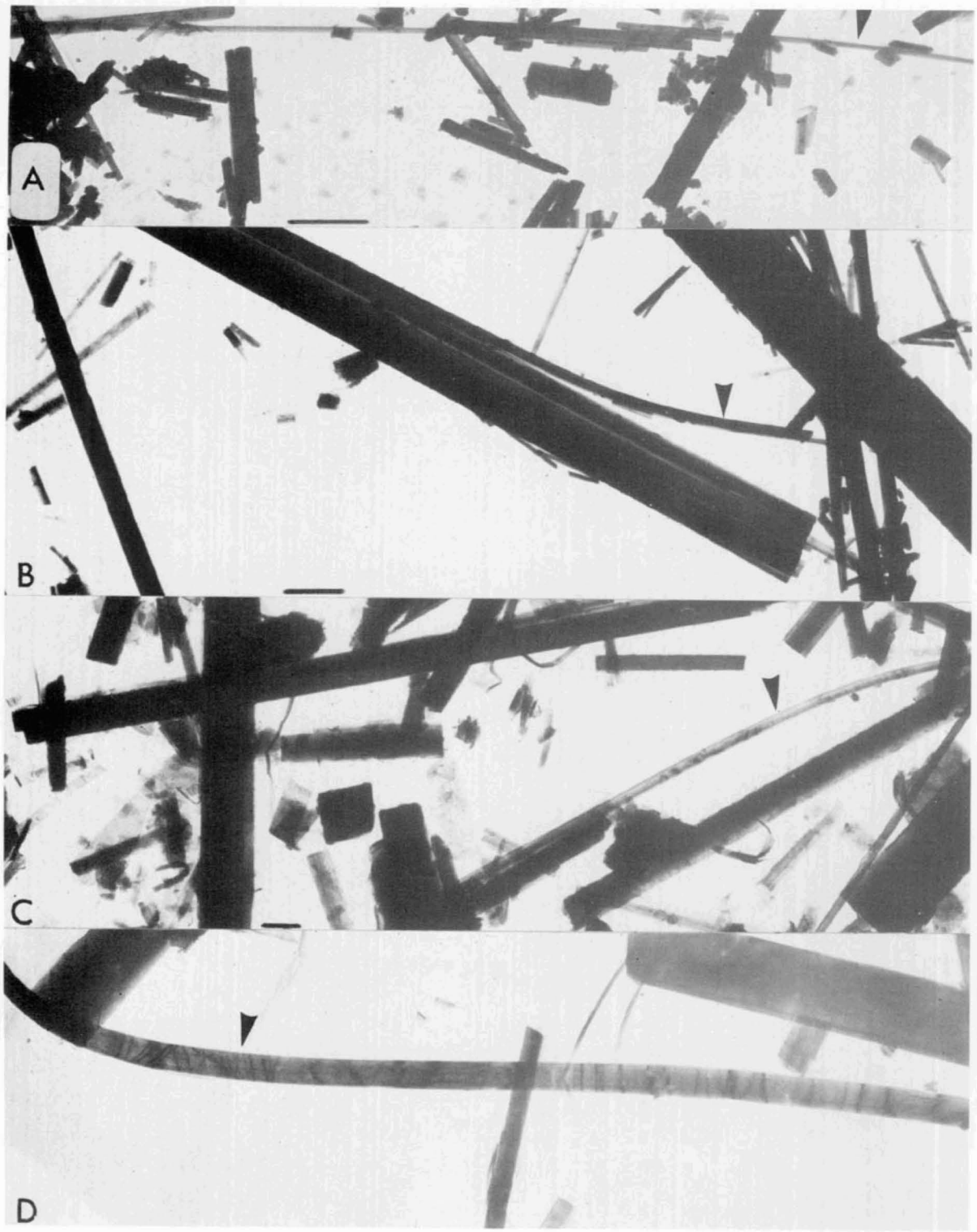

FIGURE 2. Transmission electron micrographs of amphibole asbestos showing presence of curved fibers (arrow) in *(A)* crocidolite, *(B)* amosite, *(C)* anthophyllite, and *(D)* tremolite. Bar marks equal 1 μm.

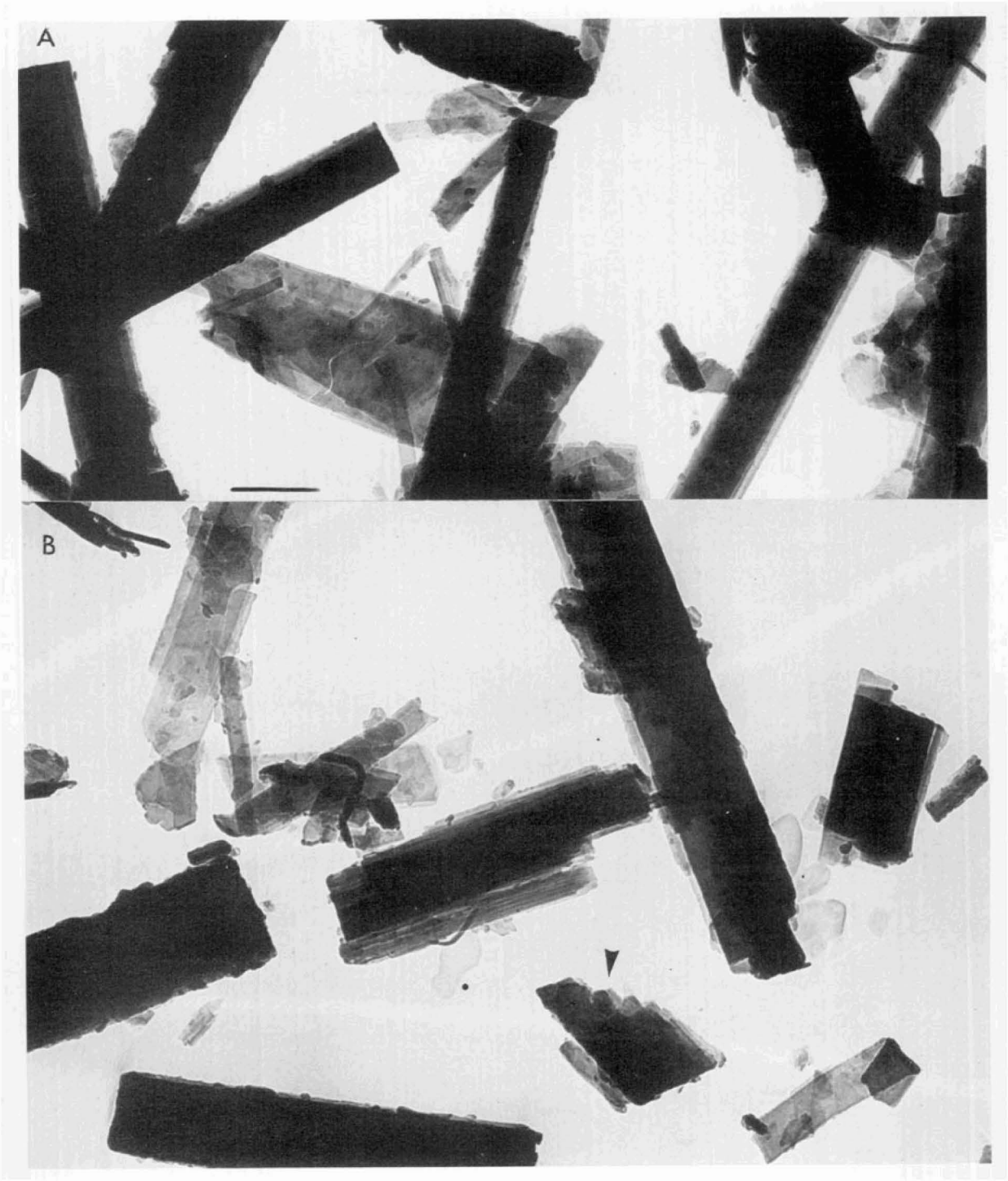

FIGURE 3. Morphological variation of amphibole asbestos fibers as illustrated by *(A)* amosite and *(B)* tremolite. Fibers range from straight-edge, right-angle fiber-axis terminations (amosite) to irregular (cleavage and fracture controlled) edges and terminations (tremolite). Arrow *(B)* shows *bc* planar view of (001) cleavage. Bar marks equal 1 μm.

fibers range from straight (right-angle termination across fiber axis) to irregular. Some irregular ends are controlled by cleavage planes parallel to the *ab* plane (Fig. 3*B*). There appears to be no general relationship between amphibole fiber type and fiber edges and cleavage. However, amosite tends to present more right-angle truncations across the fiber axis, compared to tremolite, which tends toward more prismatic forms. Anthophyllite tends to form electron translucent fibers whereas amosite tends to be more electron opaque. This latter feature is related to a number of factors including composition, density and cleavage. Internal structures, such as fine lamellae parallel to fiber axes, are common in anthophyllite but may occur in other fibers as well. Some of these features have been reported previously *(8,10)*.

Previous work concerning transmission electron microscopic examination of amphibole asbestos fibers indicated that a light and dark banding appeared to cross the fiber axis at right angles *(8)*. This banding is visible only on the electron translucent fibers. Some workers have called these bands decoration patterns in reference to similar diffraction contrast features observed on sheet silicates, especially talc *(11)*. Diffraction contrast figures have been observed on all amphibole fiber types. They tend to form continuous, curved bands across the fiber axis (Fig. 4). The nature of diffraction contrast figures in bright field imaging is well understood. Apparently, the energy absorption in the fiber is converted to heat which produces some distortion in the structure within the fiber. The result is a change in the electron diffraction path (beam to crystal plane angle) producing changes in contrast. Chrysotile, which has not been observed to flex in this manner, appears to dehydroxylate rather than deform. This is common for hydrous minerals *(12)*.

Size Distribution Characteristics of the Amphibole Fibers

The width distribution for each amphibole asbestos type was measured directly from photographic enlargements of EM plates with a resultant magnification of 7000×. Four to six plates, at the same magnification, were used to obtain values for each fiber type. Numerical data are given in Table 1. Measurements from each photographic plate were obtained with a millimeter rule which was adequate for distinction of fiber widths to 0.1 μm. Interobserver error, previously determined in another study, is small *(13)*. The heaping phenomenon was negated by interval selection at the 0.1 μm division *(13)*.

The size distribution of the amphibole asbestos minerals forms a log-normal curve strongly skewed toward the small size widths. The skewing is more marked for crocidolite and amosite than for anthophyllite and tremolite, as previously reported *(14)*. Thus, more than 50% of the crocidolite fibers are less than 0.16 μm in width, whereas only 40% of the amosite, 29% of the tremolite, and 20% of the anthophyllite fibers fall below this size range. The next most abundant size class for crocidolite and amosite lies on the smaller-size side of their modal class whereas the next most abundant size class for anthophyllite and tremolite lies on the next coarse-size side of their modes. Polymodal size distributions are common for these latter two fibers suggesting that more complex cleavage has produced more possible orientations, and concomitant viewing aspects. These variations in cross-sectional aspects have been reported previously *(10)*. Width distribution trends described here have been reported in the literature *(14)*. The data presented herein represent smaller dimensional characteristics of amphibole fiber populations than has been previously described.

Amphibole fiber lengths were measured in the same way from selected photographs (actual magnification 4,000×). Tremolite fiber was eliminated from this analysis because of its close similarity to anthophyllite with respect to length. Results are presented in Table 2.

The amphibole asbestos fibers display a range of length distribution characteristics more remarkable than their width distribution characteristics. Almost 98% of the crocidolite fibers were measured at less than 5 μm in length; amosite 84% of the fibers were less than 5 μm in length; anthophyllite, 61% of the fibers were less than 5 μm in length. Nearly two-thirds of the crocidolite fibers [illegible] 1 μm in length (Table 2).

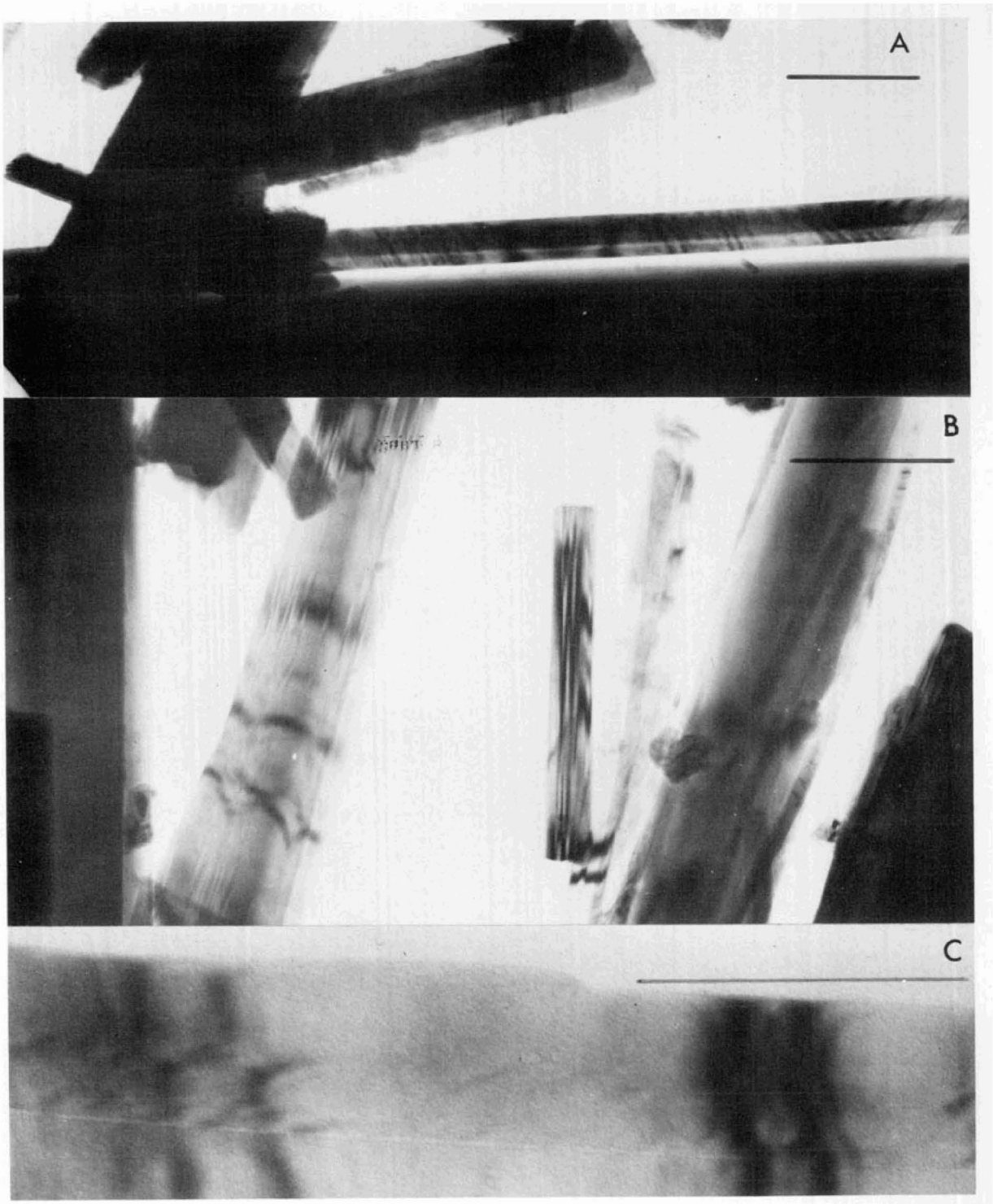

FIGURE 4. Diffraction contrast figures as illustrated by *(A)* amosite and *(B, C)* tremolite. These are observable only on thin fibers as dark bands which commonly traverse the width. These bands may be straight, curved, or angular with respect to the fiber width edge *(A)*. They may be continuous or discontinuous, apparently structurally controlled *(C)*. Rarely, they are parallel to fiber axis [see central short fiber in (B)]. These bands may be observed to move as the intensity of the electron beam varies. Bar marks in *(A, B)* equal 1 μm; bar in *(C)* is 0.5 μm.

Table 1. Width distributions of amphibole asbestos fibers.

Fiber type	No. of fibers (% of total)														
	Total N [a]	≤0.1 μm	0.11–0.2 μm	0.21–0.3 μm	0.31–0.4 μm	0.41–0.5 μm	0.51–0.6 μm	0.61–0.7 μm	0.71–0.8 μm	0.81–0.9 μm	0.91–1.0 μm	>1.0 μm	MO, μm [b]	MED, μm [c]	ME, μm [d]
Crocidolite	552	146 (26)	224 (41)	80 (15)	39 (5)	19 (5)	16	5	5	5 (8)	5	8	0.13	0.16	0.20
Amosite	192	34 (18)	74 (38)	32 (12)	19 (10)	16 (13)	3	2	5	1 (9)	1	5	0.14	0.19	0.23
Anthophyllite	261	16 (6)	62 (24)	40 (15)	33 (12)	21 (9)	31	14	15	7 (33)	5	17	0.18	0.34	0.37
Tremolite	144	26 (18)	33 (23)	29 (20)	9 (6)	12 (9)	7	12	9	4 (24)	1	2	0.17	0.25	0.37

[a] N: total number of measurements for the population.
[b] MO: modal size determined by geometrical analysis of histograms.
[c] MED: Median size determined from cumulative frequency curves.

[d] ME: Mean size calculated on the basis of central class average: $\bar{x} = \sum fx/N$. Values greater than 1.0 m were not included in the analysis. The calculated value for anthophyllite is therefore very much less than real value.

Table 2. Length distribution of selected amphibole asbestos fibers.

Fiber type	Total N	No. of fibers (% of total)						MO, μm
		<1 μm	1.1–2.0 μm	2.1–3.0 μm	3.1–4.0 μm	4.1–5.0 μm	>5.1 μm	
Crocidolite	386	243 (63)	85 (22)	30 (8)	11 (3)	7 (2)	10~0.6 (2)	
Amosite	202	46 (23)	57 (28)	44 (22)	14 (7)	8 (4)	33~1.4 (16)	
Anthophyllite	212	29 (14)	43 (20)	28 (13)	17 (8)	12 (6)	83~5.1 (39)	

Morphology of Chrysotile Asbestos Fibers

There have been numerous studies concerning the morphology of chrysotile asbestos utilizing the electron microscope. These have been reviewed *(15)*. Most of these studies have centered on the appearance of the fiber bundle and to some extent the nature of the fibril unit. The fibril has been described as possessing an internal capillary surrounded by an electron dense wall. Several of these references have shown figures of prepared chrysotile which did not possess the characteristic morphological appearance. One such study showed a ball-milled asbestos fiber which appeared to possess none of the characteristic features *(16)*. We have prepared and examined a number of chrysotile samples: (a) air-jet milled sample, sonified for preparation; (b) air-jet milled, heated at 100°C for 2 hr; (c) air-jet milled, heated at 450°C for 4 hr; (d) air-jet milled, beaten in a Waring Blendor for 30 min; (e) air-jet milled, beaten in a ballmill for 10 min. Each of these fibers were prepared in an identical manner for examination by electron microscopy. Chrysotile fibers tend to consist of bundles of fibrils which are often curvilinear with splayed ends. These features have been reported in the literature

(17). The individual unit fibrils which make up the fiber bundles are normally composed of a central capillary surrounded by an electron dense wall. Fibril dimensions range in the following manner: the central capillary, if present, ranges from 20 to 45 Å ; capillary walls range from 150 to 210 Å ; total fibril diameter from 250 to 465 Å *(17)*. Average fibril diameters range from 300 to 350 Å . Occasionally these dimensions are exceeded, but not by more than a factor of two. Characteristic chrysotile fibrils may be seen in Figure 5*A*.

The central capillary of chrysotile fibrils may vary within the same fibril, likely a function of change in viewing aspect of noncylindrical capillaries as described by Yada *(18)*. Occasionally, no central capillary is observed in the fibril, again reflecting conditions of growth *(18)*.

The normal morphology which has been ascribed to chrysotile is rarely seen when observing such material under the electron microscope. For example, we have observed that materials prepared by Waring Blendor preparation, and ball milling, bear little resemblance, other than overall fibril dimension, to the material in its natural state (Fig. 5*B,C*). Also, when chrysotile is observed for prolonged periods of time it appears to undergo deformation yielding an entirely new set of morphological characteristics.

Chrysotile fibrils normally consist of a central capillary and electron opaque walls. As time of observation increases the following morphological changes take place, in sequence: (a) the electron-dense wall decreases in width, from the outside of the fibril toward the internal capillary, yielding an electron translucent layer; (b) as the capillary wall width decreases with time, the wall and capillary bend and become deformed; (c) the central capillary may disappear (apparently collapse) yielding a contorted, much-thinned, electron dense core encapsulated in an electron translucent material which still possesses the outer fibril dimension. Features of this sequence are illustrated in Figure 6. This identical deformational series, observed with fibers prepared by heating at 100°C and 450°C, is shown in Figures 7 and 8. In addition to the alterations produced on untreated and heated chrysotile fibrils, size reduction by some vigorous mechanical methods further increases sensitivity to beam damage. For example, fiber bundle opening of chrysotile in a Waring Blendor produces irregular fibril edges (compare edges Fig. 5*A*, 5*B*). Magnesium is leached from the fiber during this process (A. M. Langer, unpublished data), which produces a weakened surface. These fibrils are readily damaged under the electron beam in extremely short time periods and display a highly deformed central capillary wall. The deformational sequence for chrysotile is such that it may be used for identification purposes.

Selected Area Electron Diffraction Characteristics of Amphibole Fibers

The electron beam interacts with atoms present in the specimen resulting in different intensities of the electron beam incident on the fluorescent viewing screen. The image of the scattered electrons is mainly related to diffraction effects and follows the Bragg geometry. Crystalline materials scatter electrons in regular patterns related to their crystal structure, atomic species present and their interplanar spacings. This image, in the back focal plane of the objective lens, may be focused on the viewing screen by defocusing the intermediate lens. The pattern obtained from an isolated particle is theoretically that of a single crystal. The reflection geometry obtained is similar to that of the Laue x-ray method (fixed crystal and film). This enables the microscopist to measure directly the d spacing dimensions and their angular relationships *(12)*.

One of us (FDP) has completed x-ray diffraction analyses of scores of amosite and crocidolite samples from South Africa. These minerals are difficult to distinguish from each other on the basis of x-ray data. These fibers are very similar in structural aspect and therefore were expected to yield similar selected area diffraction patterns. Also, because of the multiple scattering phenomenon associated with electron interaction in solids, small differences in reflection intensities disappear.

We have obtained selected area electron diffraction patterns for each of the amphibole asbestos fibers. Two representative patterns are shown in Figure 9. The normal to the horizontal

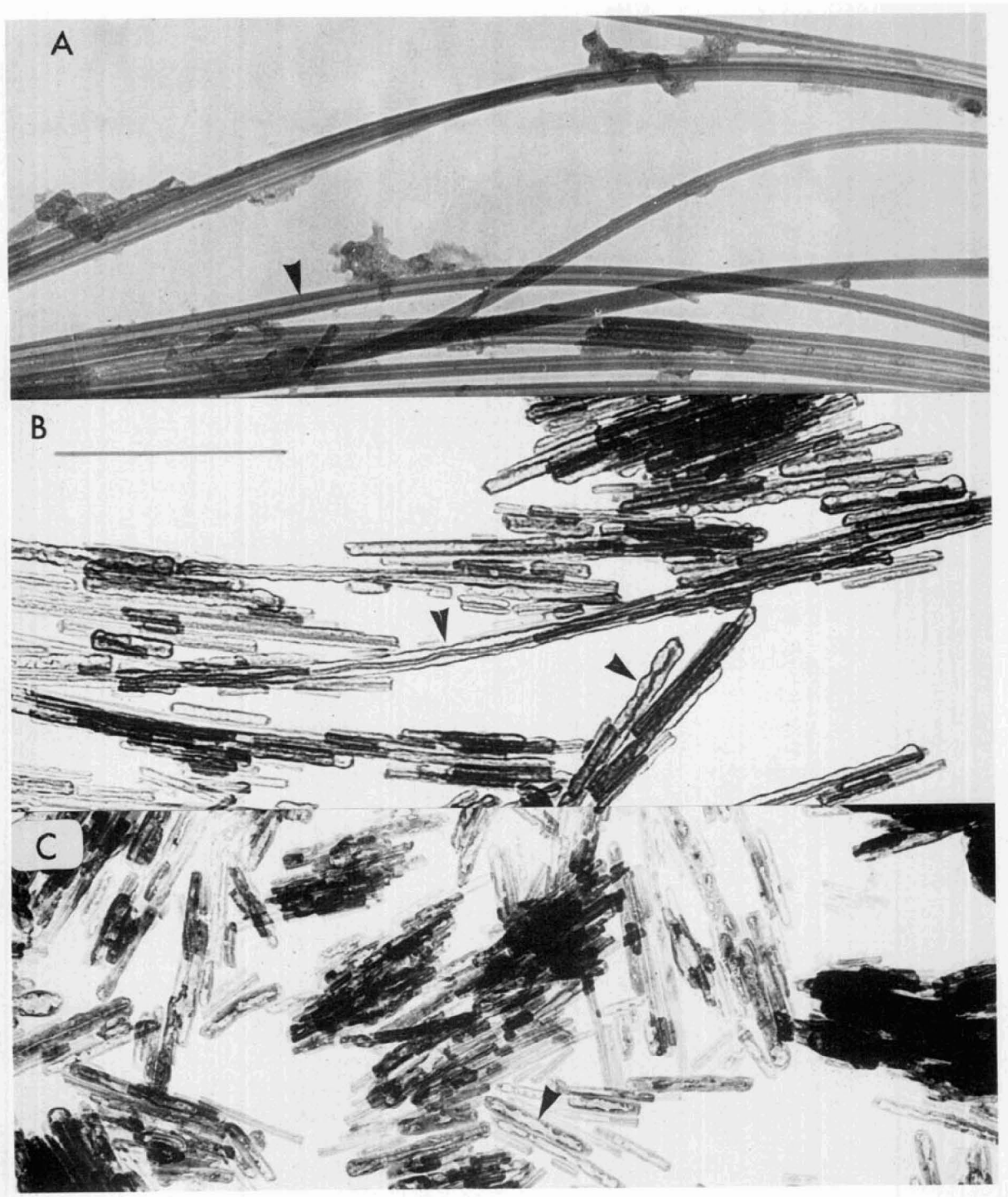

FIGURE 5. Morphology of chrysotile asbestos: *(A)* with no prior manipulation; *(B)* after beating in a Waring Blendor for 30 min; *(C)* after ball milling in a Spex Mill for 10 min. Normal morphology as viewed under the electron microscope differs after treatment. Fiber bundles are opened, reduced in length, and individual fibrils are highly sensitive to electron beam damage. Arrow in *(B)* shows electron translucent fibril with deformed and collapsed central capillary, as compared to normal fibril [arrow in *(A)*]. Ball milling tends to produce crushed fibrils [arrow in *(C)*]. Bar marks equal 0.5 μm for all photos.

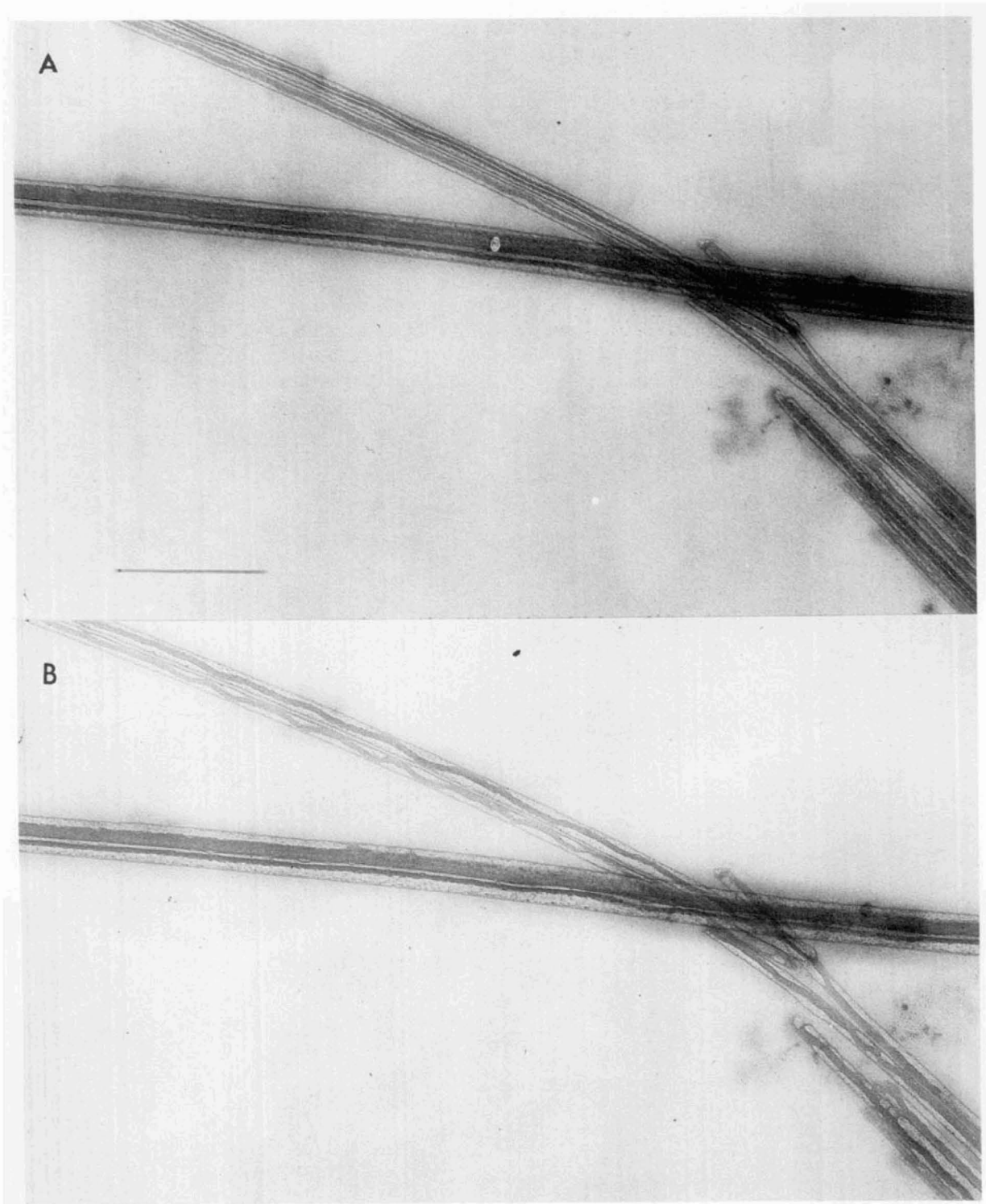

FIGURE 6. Morphological appearance of "crude" chrysotile fibers after exposure to an electron beam for *(A)* 30 sec and *(B)* 300 sec. Fibril outside diameters remain constant as the thickness of electron translucent sheath increases at the expense of the capillary wall. The internal capillary finally collapses and deforms within the fibril sheath *(B)*. Barmark in *(A)* equals 0.25 μm.

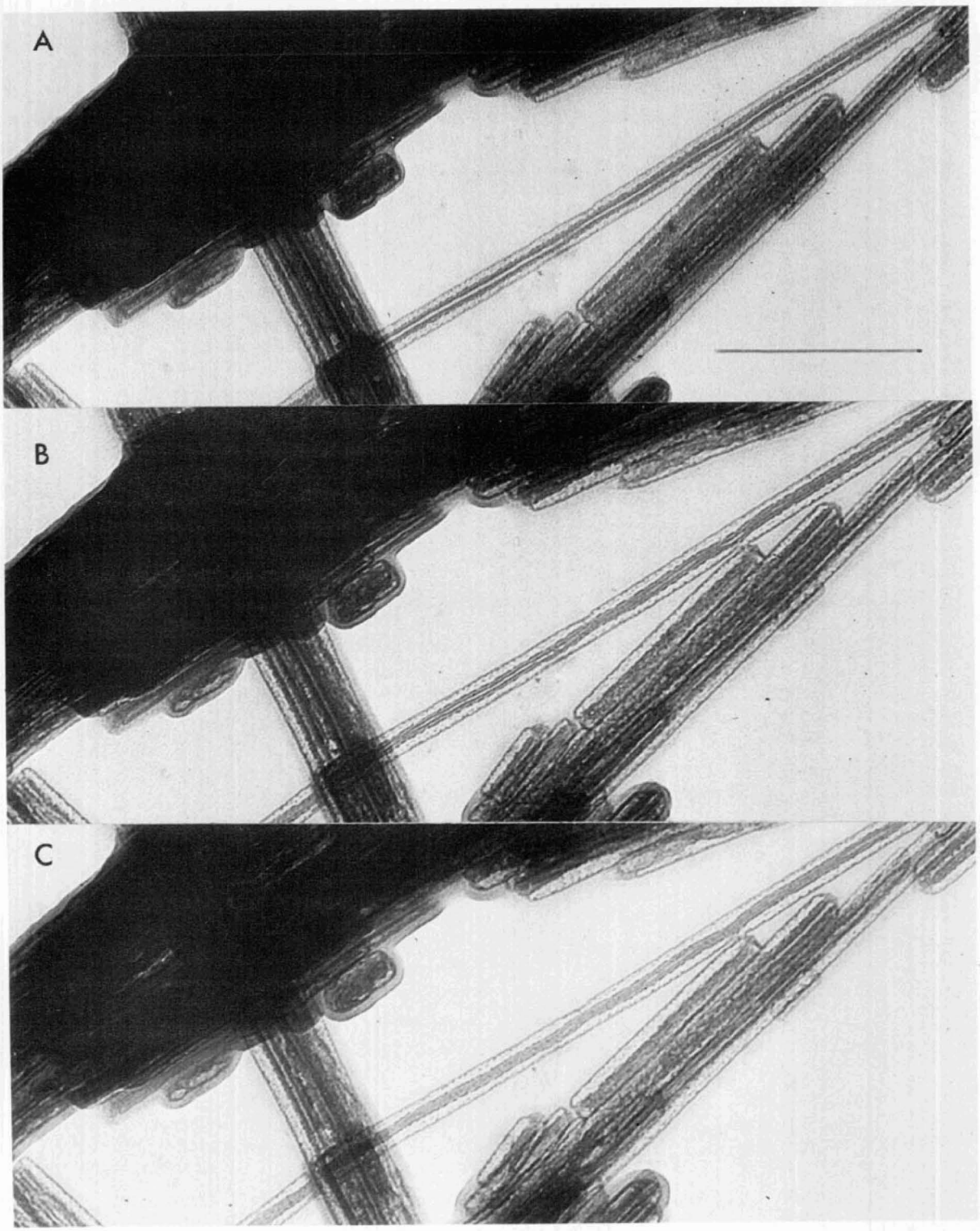

FIGURE 7. Morphological appearance of air jet-milled chrysotile fibers after exposure to an electron beam for *(A)* 20 sec, *(B)* 90 sec, and *(C)* 180 sec. The fibril deformation process is similar to that observed for crude fiber. Bar mark in *(A)* equals 0.25 μm.

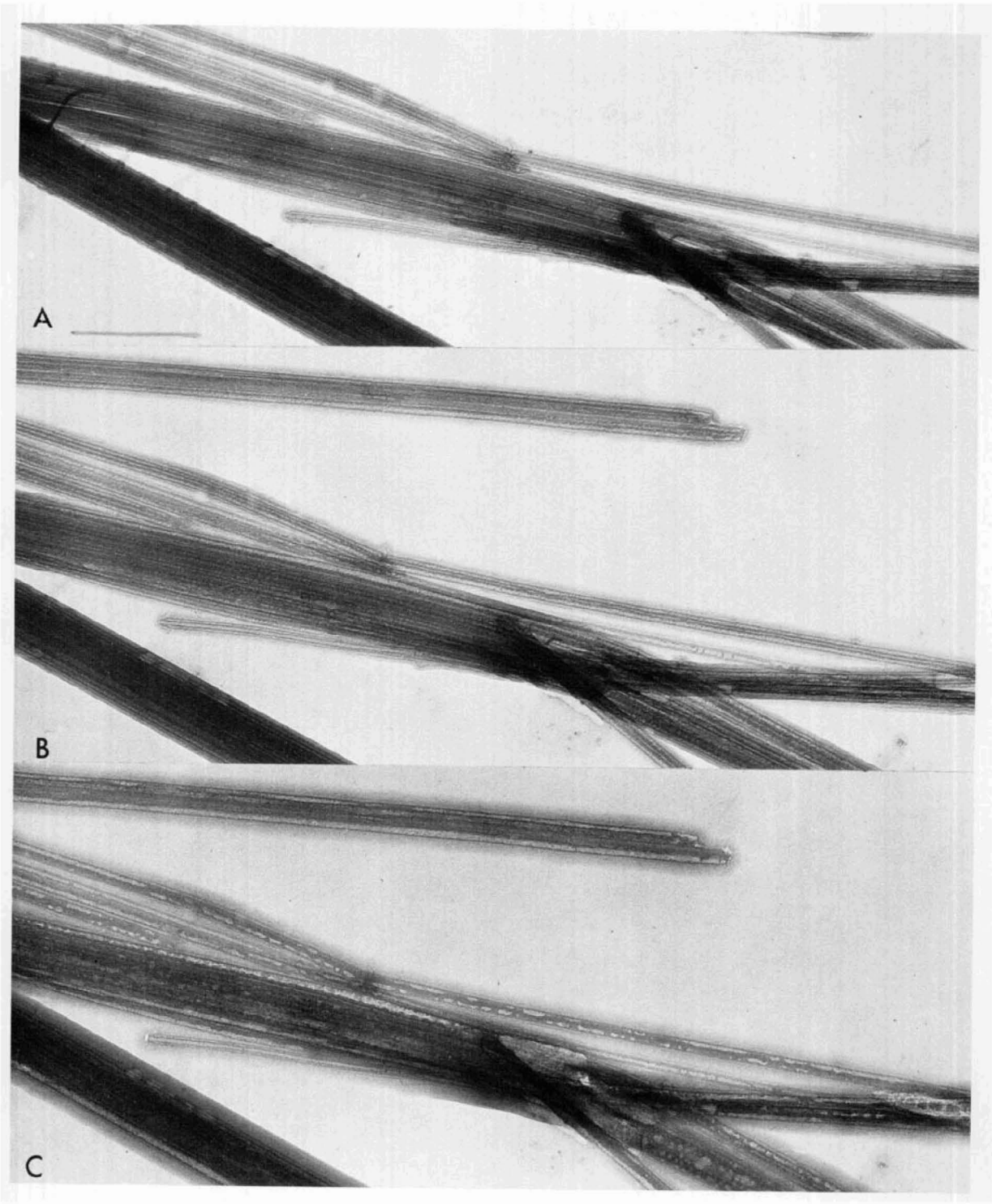

FIGURE 8. Morphological appearance of chrysotile fibers (heated at 450°C for 2 hr) after exposure to an electron beam for *(A)* 30 sec, *(B)* 120 sec, and *(C)* 720 sec. The initial fibril deformation is like the opened fiber bundles but proceeds to a form which is made up of a deformed central collapsed capillary joined to the fibril outer wall by electron dense projections *(C)*. The morphology also includes a spotty appearance suggesting some recrystallization of dehydroxylated treated materials. Bar mark in *(A)* equals 0.25 μm.

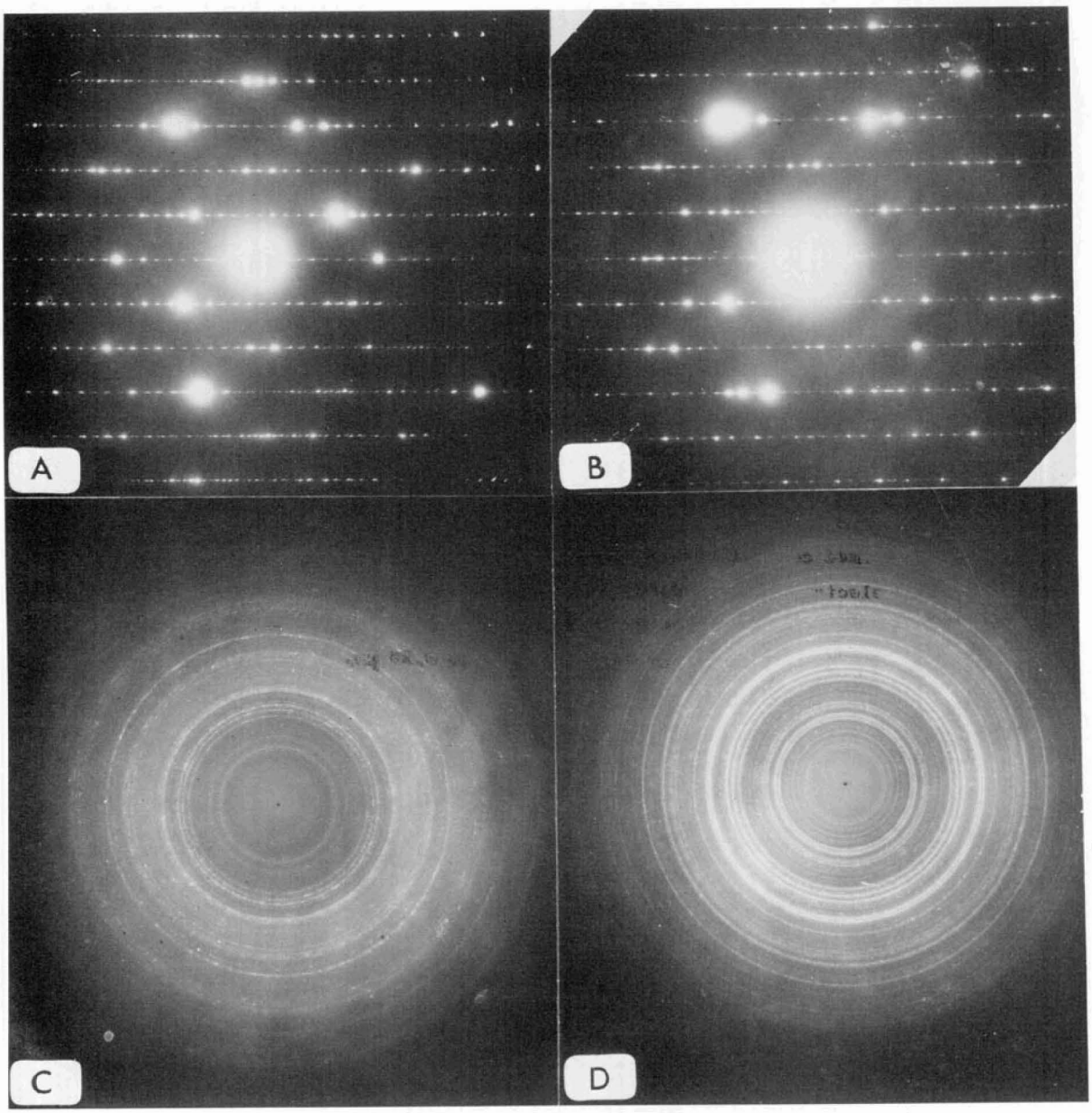

FIGURE 9. *Characteristic selected area diffraction patterns obtained on (A), (C) amosite and (B), (D) crocidolite. Patterns (A) and (B) were obtained on single fibers (single crystal pattern), whereas patterns (C) and (D) were obtained on a field of many fibers (polycrystalline pattern with Debye-Scherrer rings). The horizontal arrays (A, B) represent layer lines along the fiber reciprocal c* axis (5.3 Å for each fiber type). The spacing repeat along these rows was measured at 18.1 Å for amosite and 18.2 Å for crocidolite. These represent b* axis spacings. Their patterns are indistinguishable. The polycrystalline arrays (C, D) may be indexed as x-ray powder patterns with the precaution that both intensities and occurrence of additional reflections may confound the analysis. All patterns obtained at 75 kV.*

layer lines represents the spacing along the c^* axis of the reciprocal lattice. The c-axis dimension measured for both fiber types yielded a value of 5.3 Å . The spacings along the layer lines indicate a repeat on the order of 18.1 Å for amosite and 18.2 Å for crocidolite. These patterns are indistinguishable and represent a typical bc plane projection for amphiboles.

Obtaining diffraction patterns for accurate spacing measurements is very difficult. Clear single crystal patterns are very rare, in that the reflections tend to be multiple (double diffraction) and occasionally streaked. Quite often reflections appear that occur at fractional distances rather than in any periodicity characteristic for the amphibole space group. These features may indicate translation of symmetry elements within the structure, possibly twinning. Further complicating the electron diffraction picture, many fibers are too thick to permit the transmission of electrons while others are too thin to yield sufficient reflection reinforcement. More important, forbidden reflections tend to occur in selected area electron diffraction. That is, the amosite and crocidolite c^*-layer lines should repeat b-plane reflections only at 020, 040, 060, etc. However, there are reflections present also at 010, 030, 050, etc. For the space group $C_{2/m}$ (symmetry group for amosite and crocidolite) only $h + k$ even reflections should occur. However, both $h+k$ even and $h+k$ odd occur. There are also problems of reflections which occur with unusually great intensities. These bright spots are brought about by a multiple elastic scattering of the primary beam *(12)*. Also, the problem of particle orientation gives rise to multiple patterns for each mineral species.

The technique of selected area electron diffraction cannot be used to uniquely distinguish among single amphibole fibers. The diffraction pattern produces an array of spot reflections which may be called amphibole only. The fiber axis periodicity, along c^*, may be calculated directly from the plate utilizing the instrument camera constant. Once the c^* direction is established, the reflection array along the layer lines may be measured as well. Still, even in the best cases, results are equivocal, and microchemical characterization is required for unique identification.

Occasionally, where many fibers are in a single field a large selected area aperture may be inserted, and a polycrystalline pattern, similar in many respects to the Debye-Scherrer powder pattern, may be obtained. This has been accomplished for amosite and crocidolite (Fig. 9). Utilizing the camera constant of the instrument these rings may be measured and assigned a d spacing from within the structure. Their interpretation is again hampered by the fact that the intensities are not the same as observed for x-ray powder patterns. Although chances of identification of fibers are best in this latter case, the occurrence of so many small fibers in an area suitable for diffraction is slim.

Selected Area Electron Diffraction Characteristics of Chrysotile Fibers

Chrysotile asbestos yields a unique selected area electron diffraction pattern (Fig. 10). Layer lines which denote the periodicitv of the fiber axis a yield measurements of 5.3 Å. Reflections on these lines tend to streak parallel to the layer line which has been interpreted in x-ray diffraction studies as progressive c-axis fanning and displacement brought about by the warping of the sheet structure *(19)*. As the fiber bundles are opened, the reflections spots tend to be arcuate. These may be compared with mosaic disorientation in powder preparations in which Debye-Scherrer rings are formed. These features are relatively well defined and have been cited in the literature previously *(8, 17, 20)*. As chrysotile asbestos is progressively deformed by electron bombardment, its characteristic electron diffraction pattern changes. After 3 min a selected area diffraction pattern is observed which is markedly different from its initial character (Fig. 10).

Discussion

Identical comminution treatment of large UICC amphibole asbestos fibers produces marked differences in their size distribution characteristics. Crocidolite has a size distribution with a significant proportion of the fibers less than 1 μm in length and almost all of the fibers less than 5 μm in length. Also, over 90% of the fibers are less than 0.5 μm in width. Amosite fibers are longer and wider on the average.

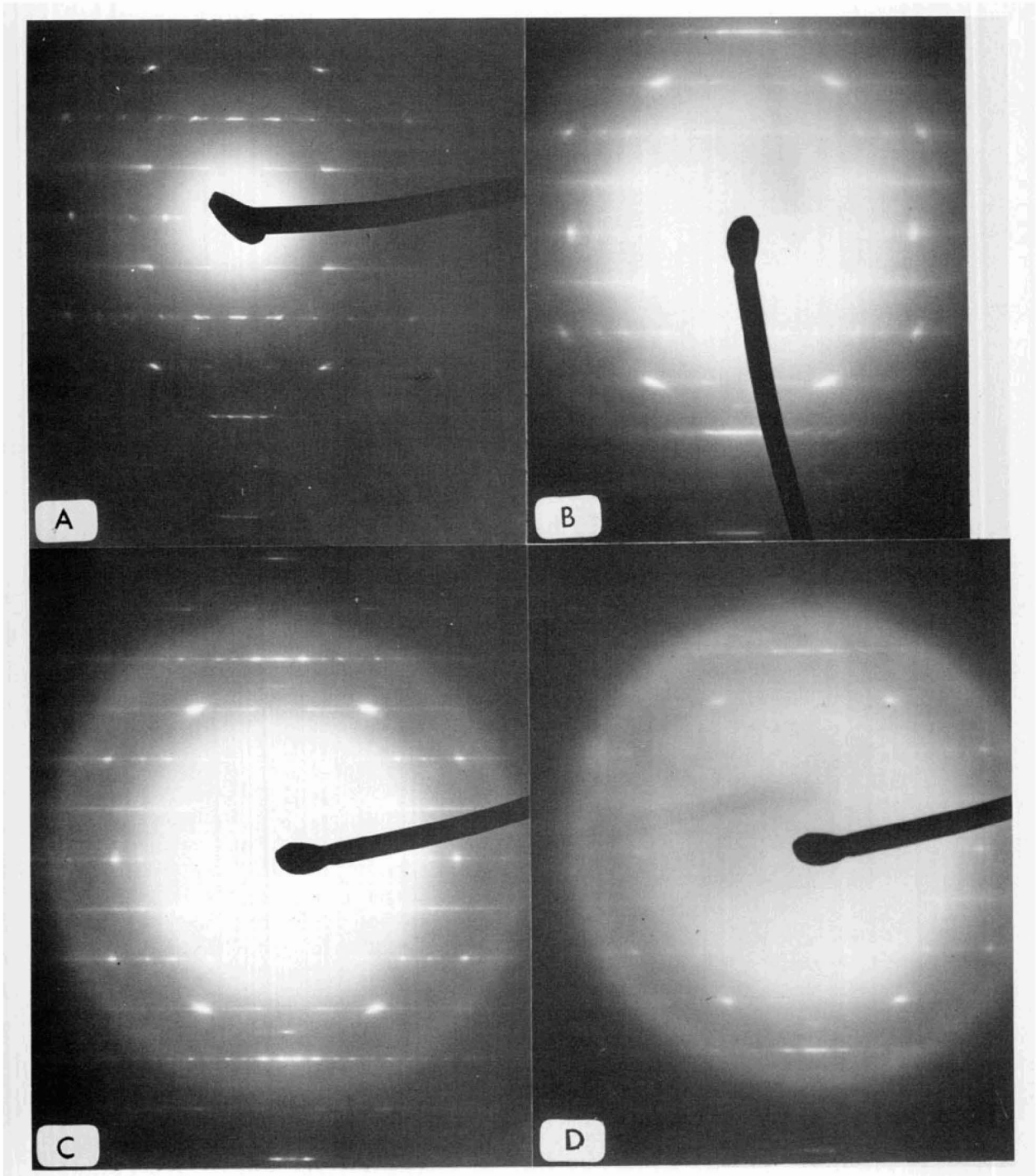

FIGURE 10. Characteristic selected area electron diffraction patterns obtained on chrysotile fibers. Pattern *(A)* represents a pattern obtained on a fiber with well ordered fibrils. The reflections in *(A)* are streaked only parallel to the layer lines (a^* axis) related only to reflections obtained from the normal cylindrical structure. The pattern on *(B)* is made up of arcs rather than streaked spots, indicating fibril disorientation (characteristic of Debye-Scherrer rings). This pattern is commonly obtained on fibers which have undergone physical manipulation during separation. Patterns in *(C)* and *(D)* represent crude fibers after *(C)* 40 sec and *(D)* 180 sec under the electron beam. The visible pattern becomes generally less intense, with high-order reflections being the first to disappear.

Anthophyllite fibers tend to be the longest and widest of the amphibole types. All other morphological and structural characteristics, and selected area electron diffraction patterns, tend to overlap.

The implications of these observations are important. For example, for a given industrial process of milling or mining, each fiber type would yield a physically different dust. Anthophyllite would yield 39 countable fibers by the NIOSH standards (a very dirty environment, in violation of the law), whereas the same mass of crocidolite would yield only two countable fibers (well within the "safe" limits) *(22)*. In terms of industrial hygiene, if a given anthophyllite process yields 39 fibers greater than 5 μm in length, measures taken to reduce fibers to the 5 fibers/ml level would significantly reduce the total mass of dust. No such dust reduction would occur in the crocidolite environment. The mass of respirable dust for each of these occupational circumstances would be vastly different.

It has been suggested that the greater disease occurrence in crocidolite miners and millers in the northwestern Cape Province, as compared to the Transvaal, is related to the fineness of the dust *(9)*. Hence, the concept of mass, surface area, particle size, and dose response is indirectly implicated in its biological importance. Also in support of the small fiber—greater biological activity theory is the observation that the largest fibers tend to accumulate in the bronchial tree, whereas the smallest fibers reach the alveolar sacs and become lodged in tissues *(14)*.

An alternative "long" asbestos fiber theory (pertaining to carcinogenic effects) would predict most disease in workmen exposed to anthophyllite dust, followed by amosite dust, and crocidolite dust. Also longer, thicker fibers from the Transvaal crocidolite fields should yield more disease stigma than that from the northwestern Cape. The opposite is true, and no data exist to support this theory. If indeed the long fibers were the most important biologically, then since fewer long fibers exist in an crocidolite population, the carcinogenicity of the individual "long" crocidolite fiber would be many magnitudes greater than for any other fiber type.

The designation of the same threshold limit value for all fibers is based on limited data. Although the absolute carcinogenicity of the various asbestos fibers is unknown, the present emphasis on crocidolite appears premature. For example, exposure to 5 fibers/ml level results in a range of mass exposures which may vary almost a magnitude for the different amphibole types. The reduction of the crocidolite exposure in Great Britain to 0.1 fibers/ml corresponds to an equivalent mass exposure for anthophyllite of 2.0 fibers/ml (based on a computation of an average particle size in which the decrease in large fibers is carried throughout the entire size range equally). The present disease patterns may result from the doses associated with each fiber type. This must be carefully studied. Within each of the amphibole asbestos types there may be a range of size distributions related to a particular mine or a particular horizon within a mine which is being worked for the ore. Cleavage parallel to the fiber axis is controlled by cation forces which occupy the M_1 and M_2 sites of the crystal lattice. These cation sites occur at the margins of adjacent opposite facing chains and provide the attractive forces which bind the chains together. A wide variety of cation species may be substituted within these sites which could change the cleavage properties of the mineral. It is important, therefore, that the various asbestos mines and mills which produce and use amphibole fibers be thoroughly studied to determine the influence of chemistry on the physical comminution of fibers. These factors may reflect the relative dust hazard.

Whereas the amphibole asbestos minerals tend to deform mechanically when bombarded with a 100 keV electron beam, chrysotile fibers are altered markedly through dehydroxylation. With a normal beam current on the order of tens of microamperes, the energy absorption from the incident electron beam may produce significant changes in the substance. Irreversible changes take place, including the production of crystal defects, atomic displacement, bond rearrangement, and all accompanying manifestations of heating. Under almost all conditions, chrysotile asbestos possesses sufficient thickness, collision cross section, and stopping power, to produce significant effects. Such isolated fibers may achieve the activation temperatures required for dehydroxylation in short periods of time. This is well documented *(12, 22)*. In addi-

tion to the thermal changes observed in more normally prepared specimens, prior treatment of the asbestos fiber leaves it even more susceptible to electron beam damage. This sequela is known and may be used for identification purposes. The selected area electron diffraction pattern of chrysotile is relatively unique. If the fiber is sufficiently thick, and has not suffered extreme electron beam damage, the selected area diffraction may be used for fiber identification. More detailed characterization of the selected area diffraction patterns of amphibole fibers needs to be done. By using a goniometer stage and well known and characterized fiber samples, it may be possible to distinguish among the amphibole asbestos types.

Although not included in this study, observations have been made that the Coalinga-type chrysotiles tend to produce more fibril-sized particles, as compared with Canadian fibers, when reduced under identical conditions. The relative proportion of respirable dust is thereby significantly greater. This may be comparable to the crocidolite fibers where disease association is most marked in areas where finer dusts are generated. An investigation into this aspect is warranted.

Acknowledgement

The authors (AML, ADM) wish to acknowledge support under an NIEHS Center Grant, ES 00928. One of us (AML) wishes to acknowledge support under an NIEHS Career Scientist Award, ES 44812.

REFERENCES

1. Bogovski, P., Gilson, J. C., Timbrell, V. and Wagner, J. C., Eds., Proceedings of the Conference on Biological Effects of Asbestos, Int. Assn. Res. Can. Scientific Pub. No. 8, Lyon, 972 WHO (1973).
2. Harries, P. G. Asbestos hazards in naval shipyards. Ann. Occup. Hyg. **11:** 135 (1968).
3. Selikoff, I. J., and Hammond, E. C. Environmental cancer in the year 2000. 7th Natl. Cancer Conf. Proc., Amer. Cancer Soc. 1973, p. 687.
4. Ehrenreich, T., et al. Les fibres d'amiante dans les poumons humains: leur signification medico-legale dans les maladies de l'environment. Arch. Malad. Prof. Med. Travail **34:** 189 (1973).
5. Speil, S., and Leineweber, J. P. Asbestos minerals in modern technology. Environ. Res. **2:** 166 (1969).
6. Whittaker, E. J. W., and Zussman, J. The characterization of serpentine minerals by x-ray diffraction. Min. Mag. **31:** 107 (1956).
7. Ernst, W. G. Amphiboles. In: Crystal Chemistry, Phase Relations and Occurrence. Springer-Verlag, New York, 1968.
8. Langer, A. M., and Pooley, F. D. Identification of single asbestos fibers in human tissues. In: Proceedings of the International Conference on Biological Effects of Asbestos. P. Bogovski, et al., Eds., IARC, Lyon, 1974, p. 119.
9. Timbrell, V. Characteristics of the UICC standard reference samples of asbestos. In: Proceedings of the International Pneumoconiosis Conference, Johannesburg. H. Shapiro, Ed. Oxford Univ. Press, London, 1970.
10. Pooley, F. D. Asbestos bodies, their formation, composition and character. Environ. Res. **5:** 363 (1972).
11. Henderson, W., et al. Talc and carcinoma of the ovary and cervix. J. Obstet. Gynecol. Brit. **78:** 266 (1971).
12. McConnell, J. D. C. Electron microscopy and electron diffraction. In: Physical Methods in Determinative Mineralogy. J. Zussman, Ed. Academic Press, New York, 1967.
13. Langer, A. M., and Mackler, A. D. Distribution of asbestos in fibers in the lung of an asbestos workman. In preparation.
14. Timbrell, V., et al. Characteristics of respirable asbestos fibres. In: Proceedings of the International Pneumoconiosis Conference; Johannesburg, H. Shapiro, Ed., Oxford Univ. Press, London, 1970, p. 120.
15. Mackler, A. D. Morphological characteristics of chrysotile asbestos. M. S. thesis, New York University, 1972.
16. Huggins, C. S. Electron micrographs of some unusual inorganic fibers. U.S. Bur. Mines. Rept., Investig. 6020 (1962).
17. Pooley, F. D. Electron microscopic characteristics of inhaled chrysotile asbestos fiber. Brit. J. Ind. Med. **29:** 146 (1972).
18. Yada, K. Study of chrysotile asbestos by a high resolution electron microscope. Acta Cryst. **23:** 704. (1967).
19. Zussman, J., et al. Electron diffraction studies of serpentine minerals. Amer. Mineral. **42:** 133 (1957).
20. Zvyagin, B. B. Electron Diffraction Analysis of Clay Minerals Structures (translated by S. Lyse), Plenum Press, New York, 1967.
21. Standard for exposure to asbestos dust. Title 29 - Labor. Chap. XVII. Occup. Safety and Health Admin. U.S. Dept. Labor. Federal Register **37:** June 7, 1972.
22. Heindenreich, R. D. Fundamentals of Transmission Electron Microscopy, Wiley, New York, 1964.